Biomedical Magnetic Induction Tomography Using Two-Arm Archimedean Spiral Coil: A Feasibility Study

Ziyi Zhang*, Peiguo Liu, Dongming Zhou, Hengdong Lei

***Abstract*—Based on the principle of primary excitation magnetic field counteraction, in this paper a new type of excitation coil named two-arm Archimedean spiral coil (TAASC) is designed and first introduced into biomedical magnetic induction tomography coil system to improve the coil system sensitivity. The primary voltage and the scaled level map of secondary voltage perturbation for the TAASC are calculated through theory and simulation. The coil system sensitivity curves when using the TAASC as excitation coil are tested at different positions, electrical conductivities and frequencies by simulation experiments. As a control, all the theoretical calculations and simulation experiments are conducted again for the circular excitation coil. The results show that the primary excitation magnetic field can be markedly counteracted while the secondary induction magnetic field perturbation is nearly at the same order of magnitude, and the coil system has a bigger sensitivity with an improvement factor of 10^3 to 10^4 by using this new type of TAASC as excitation coil, compared with the common circular excitation coil. The simulated results are in good agreement with the theoretical results.**

***Index Terms*—Biomedical magnetic induction tomography, electrical conductivity, coil system sensitivity, two-arm Archimedean spiral coil.**

I. Introduction

Haemorrhagic cerebral stroke is one of the common mortal diseases in the worldwide. Conventional diagnostic methods for haemorrhagic cerebral stroke such as magnetic resonance imaging (MRI) and computed tomography (CT) are expensive and unsuitable for real-time monitoring [1]. Because the electrical conductivity of lesion in the human brain is much higher than that of the surrounding normal tissues for haemorrhagic cerebral stroke patients, it provides the possibility to apply electrical impedance tomography (EIT) or magnetic induction tomography (MIT) technique to diagnose some pathological processes in the human brain (e.g., haemorrhagic cerebral stroke, brain oedema and brain tumor) by mapping the internal electrical conductivities of brain tissue. EIT could overcome the challenges brought by MRI and CT, but it needs to make multiple electrodes directly touch the human head, which is inaccurate for measurement and considerably uncomfortable for the patients. Compared with other imaging methods, biomedical MIT is a relativity new and promising modality due to its obvious advantages of contactless feature and low cost, and hence has the great potential for clinic application in haemorrhagic cerebral stroke detecting and monitoring [1], [2]. In biomedical MIT coil system, an alternating primary excitation magnetic field B_0 from an array of excitation coils is applied to the object under investigation. Changes of the electrical conductivity σ inside the object could cause a secondary magnetic field perturbation ΔB due to the eddy current effect induced in the object. The primary excitation magnetic field B_0 and the secondary magnetic field perturbation ΔB are then measured via an array of receiver coils in the form of primary voltage V_0 and secondary voltage perturbation ΔV, respectively. The secondary voltage perturbation ΔV which contains the information about electrical conductivity σ of the object is of interest. Taking into account the low electrical conductivity (less than 10 S/m) for biological tissues, however, the secondary voltage perturbation ΔV is very weak compared with the primary voltage V_0 and is easily submerged with V_0, i.e., the coil system sensitivity is quite low [1]–[3].

Many studies have focused on the design of receiver coil in biomedical MIT coil system to improve the coil system sensitivity, and some types of receiver coil with complex structure have been proposed, which inevitably brings much trouble in measuring signal [4]–[7]. However, up to now the excitation coil in Biomedical MIT coil system has not been fully studied. The circular coil (e.g., solenoid), which is a frequently-used type of excitation coil, has been roughly shown to be insensitive to measure the magnetic susceptibility for detection of the liver iron overload in our previous publication [8]. In order to improve the coil system sensitivity while decrease the complicacy of receiver coil and relevant signal measurement circuit, the improvement for excitation coil is required. Focusing on the property of coil system sensitivity expression, in this paper the designed two-arm Archimedean spiral coil (TAASC) which can counteract its primary excitation magnetic field by itself is first introduced into biomedical MIT coil system. The performance of TAASC is compared with that of the circular coil, and the feasibility of using TAASC as excitation coil in biomedical MIT coil system is discussed by many theoretical calculations and simulation experiments.

Manuscript received June 9, 2013. This work was supported by the Specialized Research Fund for the Doctoral Program of Higher Education of China (No. 20114307110022) from Ministry of Education of the People's Republic of China. *Asterisk indicates corresponding author*.

Z. Zhang and H. Lei are with the Department of Chemistry and Biology, College of Science, National University of Defense Technology, Changsha, Hunan 410073, China, and also with the Department of Electronic Science and Technology, College of Electronic Science and Engineering, National University of Defense Technology, Changsha, Hunan 410073, China (e-mail: ziyizhang@nudt.edu.cn; lhdandkt@gmail.com).

P. Liu and D. Zhou are with the Department of Electronic Science and Technology, College of Electronic Science and Engineering, National University of Defense Technology, Changsha, Hunan 410073, China (e-mail: peiguo_Liu@hotmail.com; dmzhou@nudt.edu.cn).

978-1-4799-3163-7/13/$31.00 ©2013 IEEE

II. METHODS

A. Sensitivity in Biomedical MIT Coil System

A simplified model of biomedical MIT coil system is shown in Fig. 1. Because the operating frequency for biomedical MIT is generally in the range of 10 kHz to10 MHz, the skin depth of object is usually large with respect to the dimensions of object. Therefore, the following relation has been proved [3], [4]

$$\frac{\Delta V}{V_0} = kf(2\pi\varepsilon_0\varepsilon_r f - j\sigma) \tag{1}$$

where k is a constant related to the relative position and geometry of the coils and object, f is the frequency of excitation current, and ε_0, ε_r, and σ are the permittivity of free space, the relative permittivity of object and the electrical conductivity of object, respectively.

The relative voltage perturbation $\Delta V/V_0$ is usually treated as the sensitivity in biomedical MIT coil system. The coil system sensitivity is an important quantity which reflects the relative variation of voltage induced in the receiver coil versus the electrical conductivity of object under investigation. For biological tissues, $\mathrm{Im}(\Delta V/V_0)$ is much larger than $\mathrm{Re}(\Delta V/V_0)$ in magnitude, so $\mathrm{Im}(\Delta V/V_0)$ plays a dominant role in the relative voltage perturbation, which contains the information about σ. However, (1) is only valid in the case of neglecting the magnetic property of object. This is suitable for most of biological tissues including the brain tissue because their relative magnetic permeability μ_r is very close to 1. But for the hepatic tissue whose μ_r could change in a relatively wide range, an additional magnetization effect induced in the volume of tissue should be considered, and this could lead to an another term associated with μ_r in $\mathrm{Re}(\Delta V/V_0)$ [8]–[10].

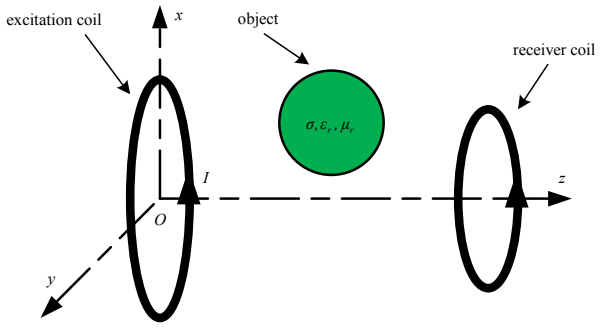

Fig. 1. Simplified model of biomedical MIT coil system.

B. Principle of Primary Excitation Magnetic Field Counteraction

The difficulty which restricts the development of biomedical MIT is largely caused by the high requirement of coil system sensitivity. It can be seen from (1) that the improvement of coil system sensitivity can be achieved if the primary voltage V_0 is decreased while the secondary voltage perturbation ΔV is kept approximately at the same order of magnitude. In other words, $\mathrm{Im}(\Delta V/V_0)$ can be increased by decreasing the primary excitation magnetic field B_0 and maintaining the secondary induced magnetic field perturbation ΔB hardly changed. Based on this principle of primary excitation magnetic field counteraction, a new type of excitation coil is designed to increase $\mathrm{Im}(\Delta V/V_0)$ in the following section.

C. Two-Arm Archimedean Spiral Coil

Focusing on the property of sensitivity expression in biomedical MIT coil system, a new type of excitation coil named two-arm Archimedean spiral coil (TAASC) [8] is developed based on the principle of primary excitation magnetic field counteraction, and is introduced into biomedical MIT coil system for the first time. As is shown in Fig. 2, the TAASC is constructed by two opposite Archimedean planar spirals connected in the origin, both of which have n turns with a maximum outer radius r_0 mm. The equations for the two Archimedean planar spirals in polar coordinate system are

$$\begin{cases} L_1: r_1 = \dfrac{r_0}{2n\pi}\varphi_1 & 0 \le \varphi_1 \le 2n\pi \\ L_2: r_2 = \dfrac{r_0}{2n\pi}(\varphi_2 - \pi) & \pi \le \varphi_2 \le (2n+1)\pi \end{cases} \tag{2}$$

The magnetic field produced by the TAASC can be regarded as the static magnetic field due to the low-frequency current flowing in it. According to the Biot-Savart law, the magnetic field produced by the TAASC could be easily calculated. If the excitation coil is circular coil, its magnetic field could be obtained similarly.

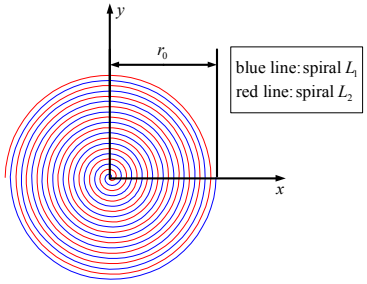

Fig. 2. Two-arm Archimedean spiral coil (TAASC).

D. Assessment Method for Level of Secondary Voltage Perturbation

The coil system sensitivity can be derived rigorously by the extensive Geselowitz theorem [11]. Here a simple and fast assessment method for the level of secondary voltage perturbation is used [12]. It is reasonable since for the weakly perturbing object in free space only the real part of ΔV contains the information about electrical conductivity σ of the object, which means that the level of $\mathrm{Re}(\Delta V)$ is of concern. $\mathrm{Re}(\Delta V)$ could be expressed as the dot product of magnetic fields produced by the excitation coil (e.g., TAASC) and the receiver coil (e.g., circular coil) with a constant factor. Although this method only offers a scaled level of the secondary voltage perturbation due to the unknown constant factor, the performance of level which is more important to us could be obtained accurately.

E. Theoretical calculations and simulation experiments description

The model for theoretical calculations and simulation experiments is based on Fig. 1. The TAASC is used as the excitation coil, placed in *x*-*y* plane with its center at the origin *O*. The current I, maximum outer radius r_0 and number of turns of TAASC are valued as 1 A, 50 mm and 1 × 2 (n = 1), respectively. The receiver coil is a circular planar coil with radius 30 mm and single turn, placed coaxially with the excitation coil. The distance between the excitation coil and the receiver coil is set as 220 mm. The homogeneous object is modeled as a small sphere with radius 5 mm, and its electrical conductivity could change from zero to 10 S/m, which covers the variation range of electrical conductivity for biological tissues well. For contrast, all the theoretical calculations and simulation experiments are conducted again, only replacing the TAASC by a circular planar single-turn coil with radius 50 mm and keeping other conditions invariable. We use commercial software (MATLAB and CST EM STUDIO) to make theoretical calculations and simulation experiments, respectively.

III. Results

A. Distribution Maps of Primary Excitation Magnetic Fields

The theoretical distribution maps of z component of primary excitation magnetic fields produced by the TAASC and circular coil in the plane of receiver coil (z = 220 mm) are shown in Fig. 3. The calculation region in the plane of receiver coil is: –30 mm ≤ x ≤ 30 mm, –30 mm ≤ y ≤ 30 mm. The theoretical magnitudes of primary magnetic flux through the receiver coil are 4.1 × 10^{-10} Wb for the circular coil and zero for the TAASC, respectively. When the frequency of current in the excitation coil is set as 100 kHz, the simulated magnitudes of primary magnetic flux through the receiver coil are 1.3 × 10^{-11} Wb for the circular coil and 4.5 × 10^{-15} Wb for the TAASC respectively, and the corresponding simulated magnitudes of primary voltage V_0 induced in the receiver coil are 8.1 × 10^{-6} V for the circular coil and 2.8 × 10^{-9} V for the TAASC respectively.

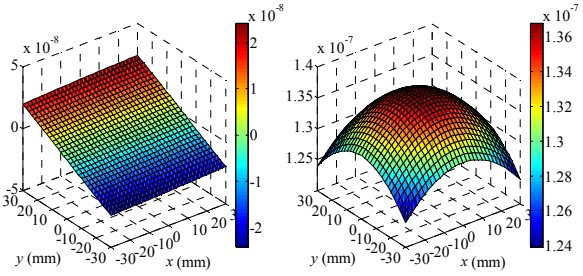

Fig. 3. Theoretical distribution maps of z component of primary excitation magnetic field produced by the TAASC (a) and the circular coil (b) at the position of receiver coil (z = 220 mm).

B. Theoretical Scaled Level Maps of Secondary Voltage Perturbation

As shown in Fig. 4(a) and Fig. 4(b), the theoretical scaled level maps of the secondary voltage perturbation when using the TAASC and the circular coil as excitation coils are calculated, respectively. The calculation region is in the plane x = 0 with –100 mm ≤ y ≤ 100 mm and 10 mm ≤ z ≤ 210 mm. In Fig. 4, both of the level maps are scaled to the maximum level value which is obtained when the excitation coil is circular coil.

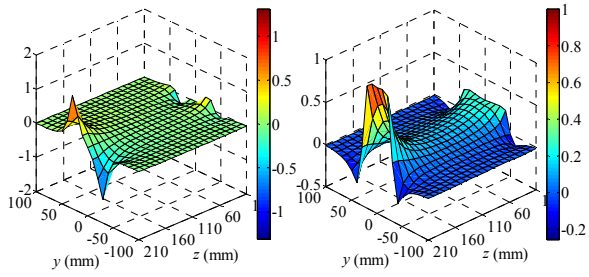

Fig. 4. Theoretical scaled level maps of the secondary voltage perturbation induced in the receiver coil when using the TAASC (a) and the circular coil (b) as excitation coils.

C. Real Part of Secondary Voltage Perturbation versus Position of Object

Fig. 5 shows the simulated results of Re(ΔV) versus the y and z positions of object. The frequency of excitation current and the electrical conductivity of object are set as 100 kHz and 6 S/m, respectively. The simulated curves in Fig. 5(a) are obtained by moving the object along the straight line of x = 0, z = 30 mm, –50 mm ≤ y ≤ 50 mm, and the simulated curves in Fig. 5(b) are obtained by moving the object along the straight line of x = 0, y = 0, 10 mm ≤ z ≤ 210 mm.

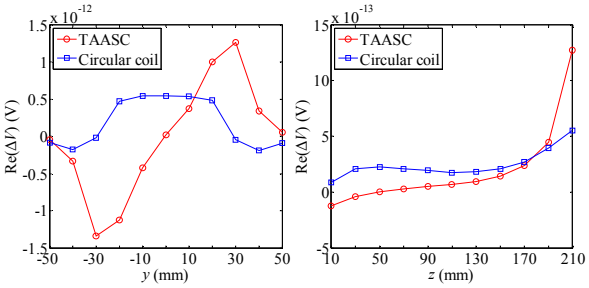

Fig. 5. Simulated results of Re(ΔV) versus the y position (a) and z position (b) of object.

D. Imaginary Part of Relative Voltage Perturbation versus Electrical Conductivity of Object and Frequency of Excitation current

The simulated results of Im($\Delta V/V_0$) versus the electrical conductivity σ of object and the frequency f of excitation current are shown in Fig. 6(a) and Fig. 6(b), respectively. The solid curves are obtained when the object is positioned at the point of x = 0, y = 30 mm, z = 210 mm, and the dashed curves are obtained when the object is positioned at the point of x = 0, y = 30 mm, z = 110 mm. In Fig. 6(a) the frequency of excitation current is set as 100 kHz and the electrical conductivity of object could change from 2 S/m to 10 S/m. In Fig. 6(b) the electrical conductivity of object is set as 6 S/m and the frequency of excitation current could change in the range of 10 kHz to 10 MHz.

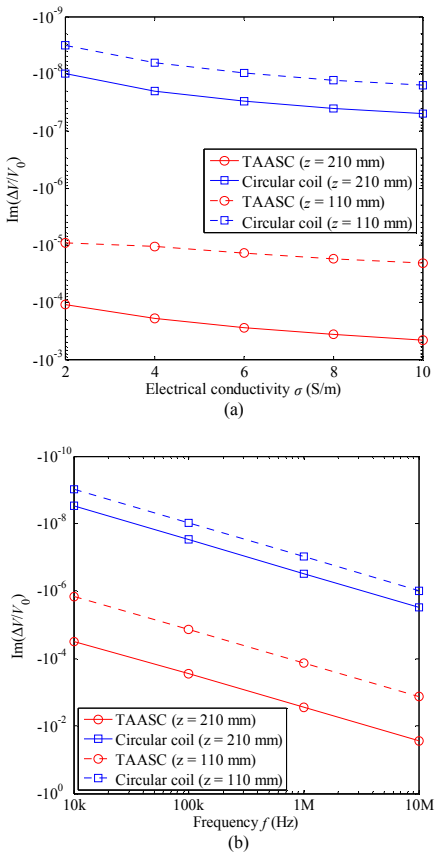

Fig. 6. Simulated results of $\mathrm{Im}(\Delta V/V_0)$ versus the electrical conductivity σ (a) of object and the frequency f (b) of excitation current.

IV. Discussions and Conclusions

From Fig. 3 it can be seen that the primary excitation magnetic field is counteracted successfully using the TAASC as excitation coil, compared with the circular excitation coil. Because the distribution of z component of primary excitation magnetic field produced by TAASC is anti-symmetric at the position of receiver coil, the theoretical magnetic flux through the receiver coil is null. However, due to the calculation errors from simulation software, the simulated magnetic flux and induced voltage are not zero for the TAASC. In our simulation experiments, the primary voltage induced by the TAASC is 3 to 4 orders lower than that induced by the circular coil.

Fig. 4 shows that the theoretical scaled real part of secondary voltage perturbation induced in the receiver coil is maximum at the point of $x = 0$, $y = 30$ mm, $z = 210$ mm in the calculation region, when using the TAASC as excitation coil. Its maximal value for the circular excitation coil is at the point $x = 0, y = 0, z = 210$ mm. Both the two maximum values are at the same level with a ratio about 1.3. In Fig. 5, the simulated results for the real part of secondary voltage perturbation versus the position of object are in good agreement with the theoretical results, showing the positions of maximum value for the TAASC is near the point $x = 0$, $y = 30$ mm, $z = 210$ mm and for circular coil is near the point $x = 0$, $y = 0$, $z = 210$ mm, respectively. The ration between the simulated maximum values is about 2.3, which is close the theoretical result.

As shown in Fig. 6, under the same conditions the coil system sensitivity could be improved dramatically by using the TAASC as excitation coil, nearly 4 orders higher than the circular excitation coil. The simulated results also validate (1) that the relation curves between $\mathrm{Im}(\Delta V/V_0)$ and electrical conductivity σ, and frequency f are both linear well. For the TAASC the simulated coil system sensitivity at the position of $x = 0$, $y = 30$ mm, $z = 210$ mm is about 10 times higher than that at the position of $x = 0$, $y = 30$ mm, $z = 110$ mm.

In conclusion, compared with the circular excitation coil, the two-arm Archimedean spiral coil (TAASC) can largely counteract its primary excitation magnetic field and maintain the secondary induction magnetic field perturbation at the same level. It provides better performance than the circular excitation coil in coil system sensitivity, which can effectively improve the coil system sensitivity by a factor of 10^3 to 10^4. Therefore, it is much promising to apply the TAASC into Biomedical MIT. Further studies focusing on the weakly perturbing within conducting background will be considered.

References

[1] B. Dekdouk, "Image reconstruction of low conductivity material distribution using magnetic induction tomography," Ph.D. dissertation, Dept. Elect. Electron. Eng., Manchester Univ., Manchester, UK, 2011.

[2] H.-Y. Wei and M. Soleimani, "Electromagnetic tomography for medical and industrial applications: challenges and opportunities," *Proc. IEEE*, vol. 101, pp. 27–46, Mar. 2013.

[3] H. Griffiths, "Magnetic induction tomography," *Meas. Sci. Technol.*, vol. 12, pp. 1126–1131, Aug. 2001.

[4] H. Griffiths, W. R. Stewart and W. Gough, "Magnetic induction tomography: a measuring system for biological tissues," *Ann. N.Y. Acad. Sci.*, vol. 873, pp. 335–345, Apr. 1999.

[5] H. Scharfetter, H. K. Lackner and J. Rosell, "Magnetic induction tomography: hardware for multi-frequency measurements in biological tissues," *Physiol. Meas.*, vol. 22, pp. 131–146, Feb. 2001.

[6] S. Watson, A. Morris, R. J. Williams, H. Griffiths and W. Gough, "A primary field compensation scheme for planar array magnetic induction tomography," *Physiol. Meas.*, vol. 25, pp. 271–279, Feb. 2004.

[7] H. Scharfetter, R. Merwa and K. Pilz, "A new type of gradiometer for the receiving circuit of magnetic induction tomography (MIT)," *Physiol. Meas.*, vol. 26, pp. S307–S318, Apr. 2005.

[8] Z. Zhang, P. Liu, L. Ding and L. Zhang, "A new type of excitation coil for measurement of liver iron overload by magnetic induction method," in *Proc. 5th Int. Conf. BioMedical Engineering and Informatics*, Chongqing, China, 2012, pp. 679–683.

[9] H. Scharfetter, R. Casañas and J. Rosell, "Biological tissue characterization by magnetic induction spectroscopy (MIS): requirements and limitations," *IEEE Trans. Biomedical Engineering*, vol. 50, pp. 870–880, Jul. 2003.

[10] R. Casañas, H. Scharfetter, A. Altes, A. Remacha, P. Sarda, J. Sierra, R. Merwa, K. Hollaus and J. Rosell, "Measurement of liver iron overload by magnetic induction using a planar gradiometer: preliminary human results," *Physiol. Meas.*, vol. 25, pp. 315–323, Feb. 2004.

[11] R. J. Mortarelli, "A generalization of the Geselowitz relationship useful in impedance plethysmographic field calculations," *IEEE Trans. Biomedical Engineering*, vol. 27, pp. 665–667, Nov. 1980.

[12] J. Rosell, R. Casañas and H. Scharfetter, "Sensitivity maps and system requirements for magnetic induction tomography using a planar gradiometer," *Physiol. Meas.*, vol. 22, pp. 121–130, Feb. 2001.